Contribution from the Department of Chemistry,
The University of Michigan, Ann Arbor, Michigan 48109

Metal-Metal Multiple Bonds. 5. Molecular Structure and Fluxional Behavior of Tetraethylammonium μ-Cyano-bis(cyclopentadienyldicarbonylmolybdate)(*Mo-Mo*) and the Question of Semibridging Carbonyls

M. DAVID CURTIS,* KYOUNG R. HAN, and WILLIAM M. BUTLER

Received December 28, 1979

$Cp_2Mo_2(CO)_4$, a molecule containing a Mo≡Mo triple bond, reacts with 1 equiv of cyanide ion to give an adduct which was isolated as the tetraethylammonium salt. The crystal structure of this salt has been determined by X-ray diffraction, and the cyanide ion is shown to bridge the Mo-Mo bond in an η^2 fashion wherein two electrons are donated to one Mo from the CN σ pair and two are donated to the other Mo from the CN π bond. The implication of this structure on the question of similar electron donation by semibridging carbonyls is discussed. The $Cp_2Mo_2(CO)_4(\mu\text{-}CN)^-$ ion is fluxional in solution, and it is postulated that the cyanide group exchanges its orientation by a "windshield wiper" motion with an activation energy E_a = 10.4 (±0.4) kcal/mol. Consistent with this interpretation, the cyanide positions in the solid state are also disordered in a similar manner. The crystal data are a = 10.831 (3) Å, b = 13.811 (4) Å, c = 16.580 (5) Å, β = 100.2 (2)°, V = 2441 Å^3, and Z = 4 (monoclinic, space group $P2_1/C$ (No. 14)). The structure was solved by using 2591 reflections with $I > 3\sigma(I)$ and refined to conventional indices R_1 = 0.055 and R_2 = 0.062. Some relevant molecular dimensions are as follows: Mo1-Mo2, 3.139 (2) Å; Mo2-C3N3, 1.94 Å; Mo1-C(3A)N(3A), 1.96 Å; Mo1···C3, 2.42 Å; Mo1···N3, 2.46 Å; Mo2···C3A, 2.32 Å; Mo2···N3A, 2.60 Å; Mo-CO, 1.96 Å; Mo-C(Cp), 2.35 Å; C-O, 1.14 Å; C-C(Cp), 1.40 Å; Mo1-Mo2-C3N3, 50.5°; Mo2-Mo1-C(3A)N(3A), 47.6°.

Introduction

The complex $Cp_2Mo_2(CO)_4$, which contains a Mo≡Mo triple bond, has been shown to have a rich chemistry associated with the triple bond.[1,2] Thus, a variety of soft nucleophiles displace the π bonds according to eq 1 (M = $CpMo(CO)_2$), and acetylenes react as shown in eq 2. In all cases examined

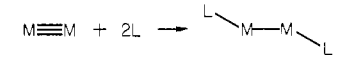
(1)

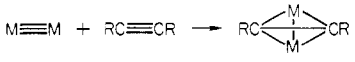
(2)

to date, added ligands donate a total of 4 electrons to the dimolydenum complex, thus maintaining the 18-electron count around each Mo atom.

It was therefore somewhat surprising to find that cyanide ion reacts with $Cp_2Mo_2(CO)_4$ to give a dark green complex in which only one cyanide ion had added to the Mo dimer (eq 3).[1] A priori, cyanide could act as a four-electron donor in

$$Cp_2Mo_2(CO)_4 + CN^- \rightarrow Cp_2Mo_2(CO)_4(CN)^- \quad (3)$$

one of two fashions—as in **1** similar to the bonding found for

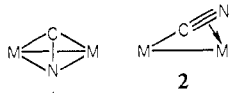
1

2

acetylenes[1,3] or as in **2** which is similar to the bonding found for the dimethylcyanamide adduct.[4] At room temperature, the ^{1}H NMR of the cyanide adduct shows only one sharp Cp resonance, consistent with structure **1**. However, a singlet could arise from some fluxional process of structure **1** or from a freak magnetic equivalence. Hence, the solid-state structure of the cyanide adduct and its temperature-dependent NMR were determined.

Experimental Section

The tetraethylammonium salt of the cyanide adduct was prepared as described previously.[1] Crystals were grown from an acetone solution saturated at 0 °C and then cooled slowly to −10 °C. A chunky crystal was affixed to a glass fiber and mounted on a Syntex $P2_1$ diffractometer (see Table I for relevant statistics). Initial rotation photographs and counter data indicated the crystal to be monoclinic, space group $P2_1/C$ (No. 14), and the measured density gave Z = 4. A Patterson map revealed the location of the two Mo atoms. Their positions and the scale factor were refined once (R = 29%), and the difference map yielded the location of all nonhydrogen atoms. Refinement of all positional and isotropic thermal parameters converged in two cycles (all refinements are full matrix) and then converged in two more cycles (R = 6.2%) with all atoms anisotropic. At this point 21 H atoms were located and included in the structure factor calculations but were not refined. Also, the difference maps and large thermal parameters associated with the CN group suggested a disorder of the type shown schematically in **3**; i.e., the CN group appeared

Table I. Summary of Crystallographic Statistics

a, Å	10.831 (3)
b, Å	13.811 (4)
c, Å	16.580 (5)
β, deg	100.20
V, Å^3	2441 (4)
Z	4
ρ_{obsd}, g cm^{-3}	1.62
ρ_{calcd}, g cm^{-3}	1.60
space group	$P2_1/C$
cryst dimens, mm	0.16 × 0.15 × 0.14
radiation	Mo Kα (monochromatized from graphite)
takeoff angle, deg	4
μ, cm^{-1}	10.3
transmission factors	0.85 (min), 0.89 (max)
scan speed, deg/min	2-12 (variable)
scan range	Mo $K\alpha_1$ − 0.8° to Mo $K\alpha_2$ + 0.8°
bkgd/scan time	0.8
std reflctns	064, 602, 771 (measd every 50 peaks)
2θ limit, deg	50
reflctns	5058 total, 2591 ($I > 3\sigma(I)$)
R_1	0.055
R_2	0.062
$[\Sigma w(\lvert F_o\rvert - \lvert F_c\rvert)^2/(NO - NV)]^{1/2}$	1.73

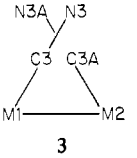
3

to lie in two overlapping orientations. A refinement in which only the population of C3-N3 was varied was then carried out and resulted in the populations of C3, N3 going from 1.0 to 0.88 and 0.78, re-

(1) Curtis, M. D.; Klingler, R. J. *J. Organomet. Chem.* **1978**, *161*, 23.
(2) Chisholm, M. H.; Cotton, F. A. *Acc. Chem. Res.* **1978**, *11*, 356.
(3) Bailey, W. I., Jr.; Chisolm, M. H.; Cotton, F. A.; Rankel, L. A. *J. Am. Chem. Soc.* **1978**, *100*, 5764.
(4) Chisholm, M. H.; Cotton, F. A.; Extine, M. W.; Rankel, L. A. *J. Am. Chem. Soc.* **1978**, *100*, 807.

0020-1669/80/1319-2096$01.00/0

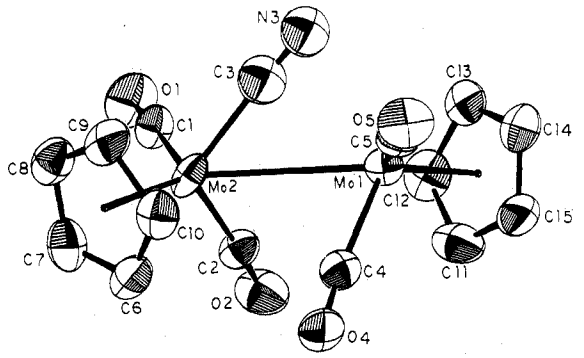

Figure 1. ORTEP plot (50% probability on thermal ellipsoids) of the ion $Cp_2Mo_2(CO)_4(\mu\text{-}CN)^-$ showing the orientation of the disordered CN group with an occupancy factor of 70%.

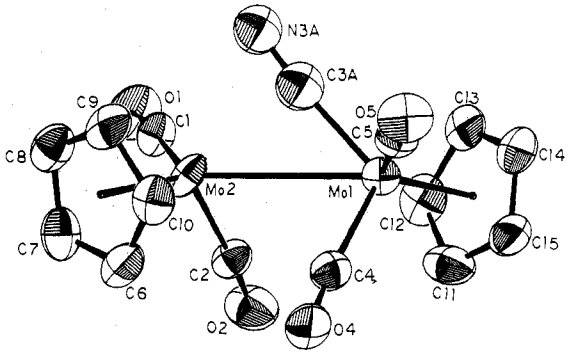

Figure 2. As in Figure 1, but showing the alternate position of the CN group with a 30% occupancy factor.

spectively. A difference map then clearly revealed the C3A, N3A positions.

The atoms C3, N3, C3A, and N3A were then put in, all at half-occupancy, and a refinement was carried out in which x, y, z, B, and the occupancy factors of these four atoms were allowed to vary. However, this model failed to refine satisfactorily (the coordinates of C3A and N3A shifted to chemically unreasonable values), but the occupancy factors (which were varied independently) suggested an occupancy factor of about 0.7 for C3, N3 and 0.3 for C3A, N3A. Several other models were tried, but none refined satisfactorily, probably because the electron density in this region is smeared due to the overlap of the orientations and due to the relatively low occupancy at the C3A, N3A sites. Consequently, the final model used set $B = 5.0$ for C3A, N3A, and their coordinates were fixed as taken directly from the difference map. The coordinates and thermal parameters of C3, N3 were allowed to vary, but the populations were set at 0.7 and 0.3 for C3–N3 and C3A–N3A, respectively. This model converged with the R values etc. shown in Table I.

The programs used in data reduction and refinement, etc., have been described previously.[5] An absorption correction was deemed unnecessary (transmission factors were calculated for a variety of crystal settings, and the extremes are given in Table I). The number of variables was 270, giving a data:variable ratio of 9.6:1. The largest peak in the final difference map was a Mo residual (2.0 e/Å^3), and the largest nonresidual peak represented 0.7 e/Å^3.

Variable-temperature ^{1}H NMR were measured in $(CD_3)_2CO$ solution at 100 MHz. Line-shape analyses were performed by using the program DNMR 3A obtained from the Quantum Chemistry Program Exchange of Indiana University.

Results

ORTEP plots showing the two orientations of the cyano ligand (70% C3–N3, 30% C3A–N3A) and the atom numbering scheme are shown in Figures 1 and 2. Figure 3 is a perspective view which shows how the cyanide group lies over the Mo–Mo bond (C3A–N3A is in essentially the same place). Figure 4 shows the tetraethylammonium ion and its numbering scheme, and Figure 5 is a stereoview of the unit cell contents. Fractional atomic coordinates are given in Table II, thermal parameters in Table III, and the bond distances and angles in Tables IV and V, respectively. The structure consists of discrete Et_4N^+ and $Cp_2Mo_2(CO)_4CN^-$ ions with no unusual intermolecular contacts.

Figure 6 shows the temperature dependent ^{1}H NMR spectrum in the Cp region of the $Cp_2Mo_2(CO)_4CN^-$ ion. The spectra on the right were computed for a two-site exchange by using the indicated first-order rate constants. A plot of ln k vs. $1/T$ gave a straight line (correlation coefficient 0.992), the slope of which yielded an activation energy $E_a = 10.4$ (±0.4) kcal/mol, and the intercept yielded a frequency factor $A = 3$ (±2) × 10^{11} s^{-1} (the error limits represent the 95% confidence levels).

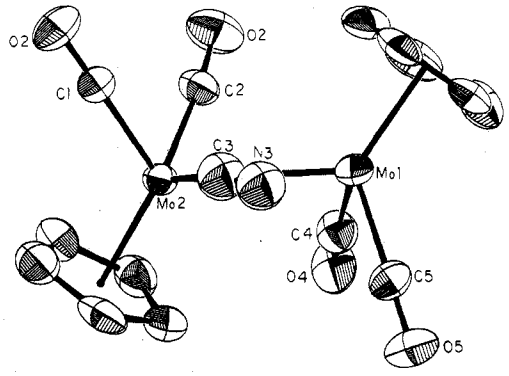

Figure 3. View of $Cp_2Mo_2(CO)_4(\mu\text{-}CN)^-$ which shows the plane of the bridging cyanide and the nearly twofold rotation symmetry of the $Cp_2Mo_2(CO)_4$ portion of the ion.

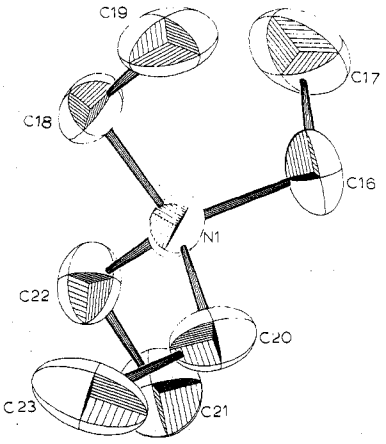

Figure 4. ORTEP plot (50% probability on thermal ellipsoids) of the tetraethylammonium ion as found in $[Et_4N][Cp_2Mo_2(CO)_4(CN)]$.

Discussion

The bonding of the cyanide ion in the adduct $Cp_2Mo_2(CO)_4CN^-$ (**4**) is seen to be such that the cyanide donates a total of four electrons to the two molybdenum atoms. Two electrons are donated in a normal (for CN^-) σ fashion, and two more are donated from the cyanide π bonds.[6] Thus, each Mo atom retains an 18-electron count if one assumes that the metal–metal π bonds of $Cp_2Mo_2(CO)_4$ are displaced upon adduct formation. The Mo–Mo distance, 3.139 (2) Å, is consistent with a Mo–Mo single-bond distance in the adduct

(5) Curtis, M. D.; Greene, J.; Butler, W. M. *J. Organomet. Chem.* **1979**, *164*, 371.

(6) Crystallographically, it is impossible to prove in the present instance that the σ bonding is through the carbon atom of the cyanide as shown in the figures rather than the alternative isocyanide structure. In view of the overwhelming frequency of M–CN bonding as opposed to M–NC bonding, the former type of bonding was chosen.

Table II. Fractional Atomic Coordinates

atom	x	y	z
Mo1	0.1565 (1)	0.2730 (1)	0.2114 (0)
Mo2	0.3195 (1)	0.0875 (1)	0.2615 (1)
C1	0.4253 (9)	0.0489 (7)	0.1838 (6)
O1	0.4911 (7)	0.0259 (6)	0.1404 (5)
C2	0.4416 (10)	0.1927 (7)	0.2683 (6)
O2	0.5205 (7)	0.2487 (6)	0.2724 (5)
C3	0.1871 (16)	0.1086 (12)	0.1682 (10)
N3	0.1038 (13)	0.1281 (10)	0.1263 (8)
C3A	0.1520 (0)	0.1420 (0)	0.1650 (0)
N3A	0.1500 (0)	0.0700 (0)	0.1300 (0)
C4	0.1996 (9)	0.2691 (8)	0.3336 (6)
O4	0.2192 (7)	0.2739 (5)	0.4028 (4)
C5	−0.0070 (9)	0.2482 (7)	0.2384 (6)
O5	−0.1047 (7)	0.2331 (6)	0.2557 (4)
C6	0.3323 (11)	0.0618 (7)	0.4022 (6)
C7	0.4071 (11)	−0.0091 (8)	0.3711 (7)
C8	0.3268 (12)	−0.0698 (8)	0.3166 (7)
C9	0.2041 (11)	−0.0378 (8)	0.3148 (6)
C10	0.2063 (10)	0.0449 (8)	0.3674 (6)
C11	0.1851 (11)	0.3469 (7)	0.0861 (6)
C12	0.3008 (11)	0.3505 (8)	0.1403 (7)
C13	0.2827 (12)	0.4067 (9)	0.2062 (7)
C14	0.1566 (11)	0.4393 (7)	0.1931 (7)
C15	0.0975 (10)	0.4009 (7)	0.1185 (7)
N1	0.7427 (7)	0.3179 (6)	0.4923 (4)
C16	0.7913 (11)	0.2165 (9)	0.5155 (7)
C17	0.7642 (15)	0.1434 (9)	0.4458 (9)
C18	0.7943 (10)	0.3569 (8)	0.4179 (6)
C19	0.9359 (11)	0.3602 (10)	0.4295 (7)
C20	0.7885 (11)	0.3835 (8)	0.5684 (6)
C21	0.7593 (12)	0.4879 (9)	0.5546 (9)
C22	0.6018 (10)	0.3196 (8)	0.4712 (6)
C23	0.5316 (10)	0.2762 (8)	0.5337 (7)
H6	0.3460 (0)	0.1260 (0)	0.4370 (0)
H7	0.4890 (0)	0.0 (0)	0.3970 (0)
H9	0.1150 (0)	−0.0650 (0)	0.2820 (0)
H10	0.1120 (0)	0.0760 (0)	0.3410 (0)
H11	0.1560 (0)	0.3100 (0)	0.0340 (0)
H12	0.3620 (0)	0.3000 (0)	0.1190 (0)
H13	0.3300 (0)	0.4320 (0)	0.2600 (0)
H14	0.1130 (0)	0.4870 (0)	0.2360 (0)
H15	0.0 (0)	0.4020 (0)	0.1040 (0)
H17	0.6600 (0)	0.1400 (0)	0.4400 (0)
H16	0.8950 (0)	0.2250 (0)	0.5340 (0)
H18	0.7460 (0)	0.4110 (0)	0.4120 (0)
H18A	0.7510 (0)	0.3120 (0)	0.3700 (0)
H19	0.9550 (0)	0.3880 (0)	0.3770 (0)
H19A	0.9900 (0)	0.2710 (0)	0.4450 (0)
H19B	0.9630 (0)	0.4010 (0)	0.4700 (0)
H20	0.7380 (0)	0.3500 (0)	0.5960 (0)
H20A	0.8600 (0)	0.3670 (0)	0.5670 (0)
H21	0.6790 (0)	0.5040 (0)	0.5500 (0)
H21A	0.7860 (0)	0.5200 (0)	0.5890 (0)
H22A	0.5710 (0)	0.3760 (0)	0.4490 (0)
H22B	0.6040 (0)	0.2900 (0)	0.4070 (0)
H23A	0.4490 (0)	0.2760 (0)	0.5020 (0)
H23B	0.5300 (0)	0.1920 (0)	0.5290 (0)
H23C	0.5710 (0)	0.2160 (0)	0.0940 (0)

(the Mo–Mo distance in $Cp_2Mo_2(CO)_6$ is 3.24 Å,[7] but bridged Mo–Mo single bonds are usually shorter[4]).

To our knowledge, the ($\sigma + \pi$) bonding mode found for the cyanide in **4** is unique to this complex although two structures have been reported in which a dialkylcyanimide, R_2NCN, bonds in a similar fashion. The relevant structural parameters involving these cyanimide ligands are shown in **5** and **6** as they appear in $Cp_2Mo_2(CO)_4(NCNMe_2)$ and $[(C_4H_8NCN)(CO)Ni]_3$, respectively.[4,8] An interesting difference in the bonding of the cyanide in **4** vs. the cyanimides in **5** or **6** is reflected in the Mo–C–N vs. the M–N–C angles. The Mo–

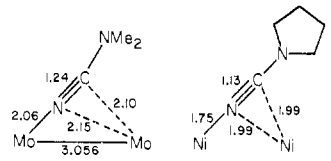

5 6

C–N angle in **4** is ca. 170° (average of Mo–C3–N3 and Mo–C3A–N3A). The M–N–C angles in **5** and **6** are much more acute, being 135 and 146°, respectively. The 170° angle in **4** is consistent with σ donation from an sp orbital on CN^-, while the smaller M–N–C angles in **5** and **6** reflect contributions from resonance form **7b** as discussed previously.[4]

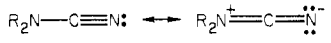

7a 7b

Unfortunately, the disorder associated with the bridging cyanide in **4** has led to difficulty in accurate atom placement. Thus, the C3–N3 distance (1.07 Å) is much shorter than the 1.15 Å usually found for cyanide complexed to metals[9] (note that the C3A–N3A distance is more reasonable). Consequently, detailed conclusions regarding the effect of the π bonding on the C–N distance cannot be made. However, even within the limitations of the present structure, it is apparent from the Mo···C and Mo···N distances (2.3–2.6 Å) that CN is a poorer π donor than Me_2NCN in **5** which exhibit Mo···N and Mo···C distances of 2.15 and 2.10 Å, respectively. However, the CN^- appears to be a better σ donor than Me_2NCN as seen by the Mo–CN distance of 1.95 Å as compared to the Mo–NCN distance of 2.06 Å in **5**.

We have previously suggested that there are two types of semibridging carbonyl groups in metal–metal bonded complexes.[10,11] The first type (**8**) was explained by Cotton et al.[12]

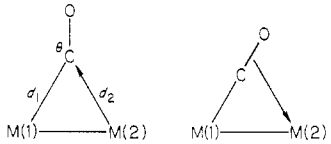

8 9

as a mechanism for relieving charge imbalance on the two metals. Thus, if M(2) in **8** is electron rich vis-á-vis M(1), then back-donation of electrons into the π^* orbitals of the semibridging CO redistributes the excess charge on M(2). This type of behavior will be referred to as "2-e donation" of the carbonyl. The second type of interaction (**9**) is postulated to involve electron donation from the CO π orbitals to M(2) and will be referred to as "incipient 4-e donation", or simply 4-e donation.

These two types of semibridging interactions may be recognized by the different behavior of θ, the M–C–O angle, with respect to α, the "asymmetry parameter", defined as $\alpha = (d_2 - d_1)/d_1$ where d_2 is the long M···C distance and d_1 is the short M–C distance. In the 2-e donation mode, θ decreases monotonically with decreasing α, whereas 4-e donation is manifested by θ being essentially invariant with respect to α.[10,11,13]

(7) Adams, R. D.; Collins, D. M.; Cotton, F. A. *Inorg. Chem.* **1974**, *13*, 1086.
(8) Krogmann, K.; Mattes, R. *Angew. Chem.* **1966**, *78*, 1064.
(9) Wells, A. F. "Structural Inorganic Chemistry"; Oxford University Press: London, 1962; p 732 ff.
(10) Klingler, R. J.; Butler, W. M.; Curtis, M. D. *J. Am. Chem. Soc.* **1978**, *100*, 5034.
(11) Curtis, M. D.; Butler, W. M. *J. Organomet. Chem.* **1978**, *155*, 131.
(12) Cotton, F. A.; Kruczynski, L.; Frenz, B. A. *J. Organomet. Chem.* **1978**, *160*, 93 and references therein.
(13) From a practical view, carbonyls with $\alpha \geq 0.6$ are essentially "terminal" and with $\alpha \leq 0.1$ are "bridging", and the "semibridging" appellation may be applied to the range of α between these two extremes with the realization that the distinction between bridging and semibridging or semibridging and terminal is very nebulous near the extremes. That is, structures of carbonyls show a smooth gradation from one extreme to the other with no discontinuities.

Table III. Thermal Parameters

atom	B_{11}	B_{22}	B_{33}	B_{12}	B_{13}	B_{23}	B,[b] Å^2
Mo1	1.90 (4)	3.23 (4)	2.50 (4)	−0.01 (3)	1.08 (3)	0.07 (3)	2.73 (2)
Mo2	4.01 (5)	1.97 (4)	3.78 (4)	−0.14 (3)	2.24 (3)	−0.26 (3)	2.73 (2)
C1	3.9 (5)	2.9 (4)	3.6 (5)	0.2 (4)	1.5 (4)	−0.0 (4)	3.3 (2)
O1	5.6 (4)	5.5 (4)	5.5 (4)	0.8 (3)	3.3 (3)	−1.1 (3)	4.6 (2)
C2	4.2 (5)	2.9 (4)	3.0 (5)	−0.6 (4)	1.1 (4)	0.1 (4)	3.2 (2)
O2	4.8 (4)	5.5 (5)	4.8 (4)	−1.8 (3)	0.1 (3)	0.6 (3)	4.8 (2)
C4	4.2 (5)	3.5 (5)	3.3 (5)	0.2 (4)	0.8 (4)	−0.1 (4)	3.6 (2)
O4	7.7 (5)	4.3 (4)	2.5 (3)	1.3 (3)	1.3 (3)	−0.6 (3)	4.1 (2)
C5	3.4 (4)	3.7 (5)	2.9 (4)	0.1 (4)	0.8 (4)	−0.6 (4)	3.2 (2)
O5	4.0 (4)	6.4 (5)	5.4 (4)	−0.7 (3)	2.3 (3)	−0.8 (3)	4.7 (2)
C6	6.4 (7)	2.9 (5)	3.6 (5)	−0.1 (4)	1.9 (5)	−0.0 (4)	3.9 (3)
C7	5.3 (6)	4.1 (6)	4.9 (6)	0.6 (5)	1.4 (5)	1.5 (5)	4.5 (3)
C8	6.4 (7)	3.0 (6)	4.1 (5)	0.0 (5)	2.0 (5)	0.3 (4)	4.1 (3)
C9	6.0 (7)	3.2 (5)	4.0 (5)	−1.4 (5)	1.7 (5)	0.6 (4)	3.9 (2)
C10	4.7 (6)	4.1 (5)	3.8 (5)	−0.0 (5)	1.8 (4)	0.9 (4)	3.9 (2)
C11	6.7 (7)	3.1 (5)	2.5 (5)	−1.0 (5)	1.2 (5)	0.7 (4)	3.5 (2)
C12	5.6 (6)	4.4 (6)	3.7 (5)	−0.5 (5)	2.6 (5)	0.8 (4)	3.9 (3)
C13	5.3 (7)	5.0 (6)	4.0 (6)	−2.3 (5)	−0.2 (5)	0.8 (5)	4.4 (2)
C14	6.0 (7)	3.1 (5)	4.4 (6)	−0.3 (5)	0.6 (5)	−0.4 (4)	4.3 (3)
C15	4.5 (5)	2.9 (5)	4.7 (6)	−0.5 (4)	1.3 (5)	1.1 (4)	3.7 (2)
N1	3.6 (4)	3.3 (4)	2.5 (4)	0.1 (3)	0.4 (3)	0.2 (3)	3.1 (2)
C16	5.7 (6)	4.3 (6)	5.3 (6)	2.1 (5)	0.5 (5)	1.4 (5)	4.7 (3)
C17	9.2 (10)	4.2 (7)	8.8 (9)	0.8 (7)	2.8 (8)	−1.2 (6)	6.7 (4)
C18	4.4 (5)	4.9 (6)	2.7 (5)	−0.0 (4)	0.6 (4)	0.6 (4)	3.8 (3)
C19	5.2 (7)	8.4 (9)	5.1 (6)	−0.6 (6)	2.8 (5)	−0.7 (6)	5.5 (3)
C20	4.6 (6)	6.3 (6)	4.1 (5)	−1.0 (5)	1.8 (4)	−1.1 (4)	4.5 (3)
C21	6.8 (7)	4.5 (7)	10.0 (9)	−1.6 (5)	3.3 (6)	−3.5 (6)	5.8 (4)
C22	3.9 (5)	3.9 (5)	4.3 (5)	−0.5 (4)	0.5 (4)	1.1 (4)	3.9 (2)
C23	4.6 (5)	5.1 (6)	5.3 (7)	−1.6 (5)	1.4 (5)	0.5 (5)	4.7 (2)
C3							5.0 (4)[a]
N3							5.5 (3)[a]
C3A							5.0 (0)[a]
N3A							5.0 (0)[a]

[a] Isotropic B value. [b] Equivalent isotropic B value.

Table IV. Bond Distances in $[Et_4N][Cp_2Mo_2(CO)_4CN]$[a]

bond	d, Å	bond	d, Å
Mo1-Mo2	3.139 (2)		
-C3A	1.96	Mo2-C3	1.94
-C4	2.00 (1)	-C1	1.94 (1)
-C5	1.93 (1)	-C2	1.95 (1)
-C3	2.42	-C3A	2.32
-N3	2.46	-N3A	2.60
-C11	2.38 (1)	-C6	2.34 (1)
-C12	2.37 (1)	-C7	2.32 (1)
-C13	2.31 (1)	-C8	2.35 (1)
-C14	2.32 (1)	-C9	2.39 (1)
-C15	2.36 (1)	-C10	2.39 (1)
Mo1-C2	3.26 (1)	Mo2-C4	3.16 (1)
C4-O4	1.13 (1)	C1-O1	1.14 (1)
C5-O5	1.16 (1)	C2-O2	1.15 (1)
C3A-N3A	1.15	C3-N3	1.07
C11-C12	1.41 (2)	C6-C7	1.42 (1)
-C15	1.39 (1)	-C10	1.40 (1)
C12-C13	1.38 (2)	C7-C8	1.41 (1)
C13-C14	1.42 (2)	C8-C9	1.40 (1)
C14-C15	1.39 (1)	C9-C10	1.43 (1)
N1-C16	1.52 (1)	C16-C17	1.52 (2)
-C18	1.54 (1)	C18-C19	1.51 (1)
-C20	1.56 (1)	C20-C21	1.49 (2)
-C22	1.50 (1)	C22-C23	1.51 (1)

[a] Standard deviation of last number in parentheses. No standard deviations are given for C3, N3, C3A, and N3A since these are grossly underestimated by the inverse matrix.

Table V. Bond Angles in $[Et_4N][Cp_2Mo_2(CO)_4CN]$

atoms	angle, deg	atoms	angle, deg
Mo1-Mo2-C3	50.5	Mo2-Mo1-C3A	47.6
-C1	114.7 (3)	-C4	72.0 (3)
-C2	75.6 (3)	-C5	106.8 (3)
-C6	108.6 (3)	-C11	115.2 (3)
-C7	144.1 (3)	-C12	96.4 (3)
-C8	146.6 (3)	-C13	110.7 (3)
-C9	112.4 (3)	-C14	146.2 (3)
-C10	93.3 (3)	-C15	149.3 (3)
C1-Mo2-C2	76.7 (4)	C4-Mo1-C5	79.6 (4)
-C3	87.2	-C3A	111.0
C2-Mo2-C3	109.4	C5-Mo1-C3A	88.1
C7-C6-C10	108 (1)	C12-C11-C15	109 (1)
C8-C7-C6	108 (1)	C14-C13-C12	109 (1)
C10-C9-C8	109 (1)	C15-C14-C13	107 (1)
C6-C10-C9	107 (1)	C11-C15-C14	108 (1)
Mo2-C1-O1	177.5 (9)	Mo1-C4-O4	174.4 (9)
-C2-O2	174.5 (9)	-C5-O5	179 (2)
-C3-N3	167	-C3A-N3A	173
C16-N1-C18	111.4 (8)	C20-N1-C22	110.1 (8)
-C20	106.4 (8)	N1-C16-C17	114.0 (9)
-C22	111.4 (8)	-C18-C19	114.5 (8)
C18-N1-C20	109.6 (8)	-C20-C21	114.2 (8)
-C22	107.9 (7)	-C22-C23	116.5 (8)

The structure of the cyanide adduct, **4**, reported here has the cyanide-donating electron density as in **9**. The values of α and θ for C3–N3 and C3A–N3A are 0.25 and 167° and 0.18 and 173°, respectively. These values place the cyanide in **4** clearly in the 4-e donation region of the published curve of α vs. θ[10] and lend support to our previous suggestion. Furthermore, incipient 4-e donation is indicated for carbonyls in a series of compounds in which a transition-metal carbonyl is metal–metal bonded to a Lewis acid, e.g., Zn, Ga, and Au. The values of α and θ of these compounds collected in Table VI show that the carbonyls are semibridging and that the M–C–O angle is essentially invariant with respect to α (the values of α and θ in Table VI also lie on the previously derived 4-e donation line in Figure 4 of ref 10).

It is hardly reasonable to suggest that the Lewis acid metal in the complexes listed in Table VI donate electrons back into the π^* level of the semibridging carbonyls. On the other hand, charge donation from the carbonyls to the Lewis acid is very

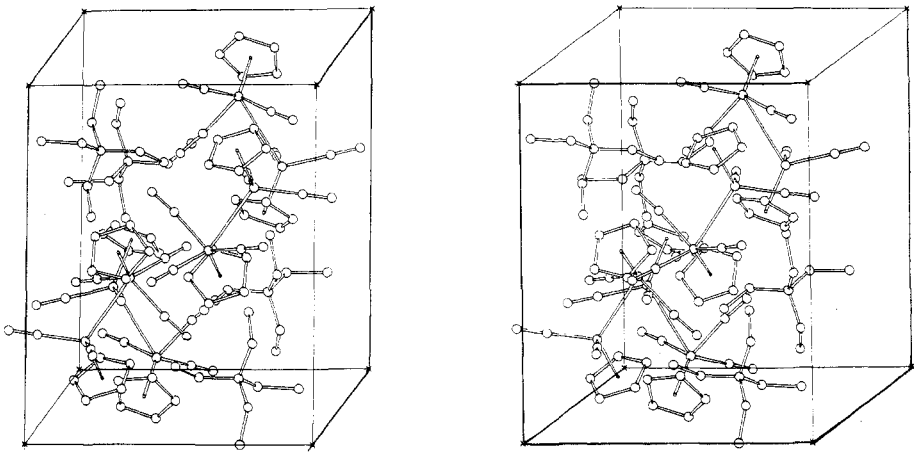

Figure 5. Stereoview of the unit cell contents of $[Et_4N][Cp_2Mo_2(CO)_4(CN)]$.

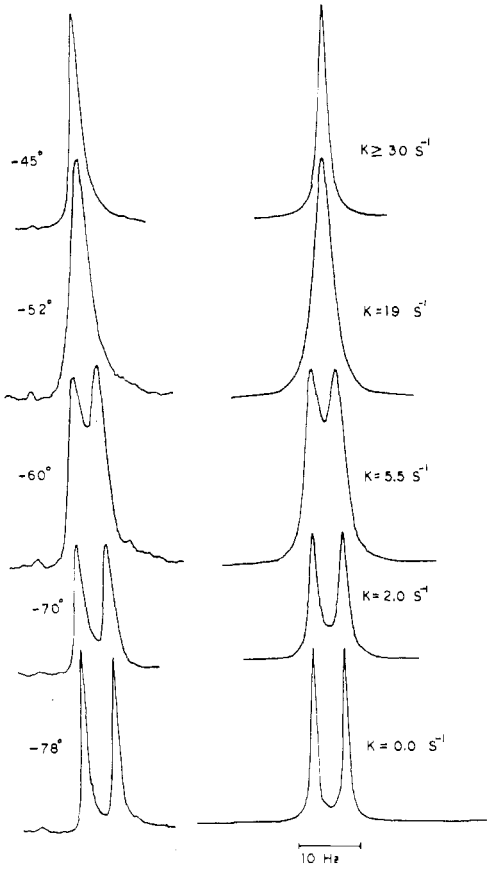

Figure 6. Observed and calculated variable-temperature ^1H NMR spectrum of $Cp_2Mo_2(CO)_4CN^-$.

likely especially in view of the fact that the strongest Lewis acids, Zn and Ga, induce the greatest degree of semibridging character in the carbonyls (lower values of α). Thus, 4-e donation seems to be experimentally established when M(2) in **9** is a Lewis acid, when M(2) would otherwise be coordinatively unsaturated (as in **4** or $(diphos)_2Mn_2(CO)_5$[14]), or when M(2) is *potentially* unsaturated due to the presence of metal–metal multiple bonds between M(1) and M(2).[15,16]

Table VI. Asymmetry Parameters for Lewis Acid Derivatives of Metal Carbonyls[a]

compd	$(d_2-d_1)/d_1$	θ, deg	ref
$CpW(CO)_3GaMe_2$	0.25, 0.38	172, 176	18
$CpMo(CO)_3ZnBr\cdot 2THF$	0.31, 0.37	174, 175	19
$[CpMo(CO)_3]_2Zn$	0.28, 0.30	175, 176	20
$[CpMo(CO)_3ZnCl\cdot Et_2O]_2$	0.30, 0.31	175, 174	20
$CpW(CO)_3AuPPh_3$	0.24, 0.41	168, 172	21

[a] The values for each of the two semibridging carbonyls are given. In those cases in which the M···C distance, d_2, was not given in the original reference, this distance was calculated from the given cell constants and atomic positions by using the bond-distance instruction of ORTEP.

The solution structure, as judged by a variable-temperature NMR study, of the cyanide adduct, **4**, appears to be the same as the solid-state structure. Below about −60 °C (Figure 6), the Cp resonance splits into a doublet as required by the inequivalency of these groups in the solid-state structure. At higher temperatures, the doublet collapses, indicating a fluxional process which causes the Cp groups to become magnetically equivalent. If the cyanide group is neglected, there is a nearly twofold rotation axis bisecting the Mo–Mo bond and passing through N3 (see Figure 3). Thus, if the cyanide flips between orientations C3–N3 and C3A–N3A via a symmetrically bridged intermediate,[17] only a slight rotation about the Mo–Mo bond is necessary to give time-averaged equivalent Cp groups. The disorder in the solid state thus appears to be a "stop-action photograph" of the fluxional process occurring in solution.[22]

(14) Colton, R.; Commons, C. J. *Aust. J. Chem.* **1975**, *28*, 1673. Commons, C. J.; Hoskins, B. F. *Ibid.* **1975**, *28*, 1663.
(15) In the last case, the metal–metal π^* orbitals are spatially situated to interact with the semibridging carbonyls, and the M–M π bond will be weakened in proportion to the extent that electrons are donated from the semibridging carbonyls.
(16) E. D. Jemmis, A. R. Pinhas, and R. Hoffmann (submitted for publication) have recently applied the EHMO method to calculate the electronic structure of $Cp_2Mo_2(CO)_4$. Although they did not address the question of bent vs. linear semibridging carbonyls, their calculations suggest a net donation from the metal to the π^* CO orbitals as proposed by Cotton.[12] Clearly the question of bent vs. linear semibridging carbonyls deserves more scrutiny.
(17) The calculations referred to in ref 16 also suggest that carbonyl scrambling via a symmetric, $CpMO(\mu\text{-}CO)_4MoCp$, structure is a low-energy process.
(18) St. Denis, J. N.; Butler, W.; Glick, M. D.; Oliver, J. P. *J. Organomet. Chem.* **1977**, *129*, 1.
(19) Crotty, D. E.; Corey, E. R.; Anderson, T. J.; Glick, M. D. *Inorg. Chem.* **1977**, *16*, 920.
(20) St. Denis, J.; Butler, W.; Glick, M. D.; Oliver, J. P. *J. Am. Chem. Soc.* **1974**, *96*, 5427.
(21) Wilford, J. B.; Powell, H. M. *J. Chem. Soc. A* **1969**, 8.
(22) A dissociative mechanism, $M_2CN^- \rightleftharpoons M_2 + CN^-$, for the exchange process is ruled out by the observation that the Cp resonance of **4** in $(CD_3)_2CO$ is unchanged upon addition of excess dimer, $Cp_2Mo_2(CO)_4$. If a dissociative mechanism were operative, the Cp resonances of **4** and excess dimer would be averaged. A bimolecular associative mechanism has not been eliminated, but is deemed to be very unlikely.

Acknowledgment. We thank Professor R. Hoffmann for providing us with a preprint.[16] We thank the donors of the Petroleum Research Fund, administered by the American Chemical Society, for the support of this research.

Registry No. $[Et_4N][Cp_2Mo_2(CO)_4(CN)]$, 69427-01-6.

Supplementary Material Available: A listing of observed and calculated structure factor amplitudes for compound **4** (10 pages). Ordering information is given on any current masthead page.

Contribution from the Departments of Chemistry, Hunter College, City University of New York, New York, New York 10021, and Colorado State University, Fort Collins, Colorado 80523

Structures and Properties of *N*-Methyltetraphenylporphyrin Complexes. Crystal and Molecular Structure and Cyclic Voltammetry of an Air-Stable Iron(II) Porphyrin: Chloro(*N*-methyl-5,10,15,20-tetraphenylporphinato)iron(II)

OREN P. ANDERSON,*[1] ALAN B. KOPELOVE,[2] and DAVID K. LAVALLEE*[2]

Received January 25, 1980

An air-stable iron(II) metalloporphyrin, chloro(*N*-methyl-5,10,15,20-tetraphenylporphinato)iron(II), has been characterized by cyclic voltammetry, and its crystal and molecular structures have been determined. Complexation with the coordinatively restrictive *N*-methylporphyrin ligand greatly stabilizes the Fe(II) oxidation state relative to Fe(III) ($E_{1/2}$ for [Fe(*N*-CH_3TPP)Cl] is +0.49 V vs. SCE while $E_{1/2}$ for [Fe(TPP)Cl] is −0.29 V). The cyclic voltammogram of the *N*-methylporphyrin complex shows reversible metal ion oxidation unlike the behavior of the nonmethylated porphyrin complex. The crystal and molecular structures of [Fe(*N*-CH_3TPP)Cl] have been determined from three-dimensional single-crystal X-ray diffraction data, collected by counter techniques. The dark blue crystals are triclinic, of space group $P\bar{1}$ (No. 2), with two formula units in the unit cell (a = 7.5620 (6) Å, b = 14.961 (2) Å, c = 17.434 (2) Å, α = 103.15 (1)°, β = 97.124 (9)°, γ = 93.84 (1)°). The structure has been refined by full-matrix least-squares methods to R = 0.043 (R_w = 0.055) for 4056 unique reflections with $F^2 > 3\sigma(F^2)$. The discrete, monomeric complexes exhibit a highly distorted square-pyramidal coordination geometry about the iron(II) atom, with the chloro ligand occupying the apical position (Fe–Cl = 2.244 (1) Å). The *N*-alkylated porphyrin ligand forms three strong bonds to the iron(II) atom (Fe–N2 = 2.118 (2) Å, Fe–N3 = 2.116 (2) Å, Fe–N4 = 2.082 (2) Å), together with one weaker bond (Fe–N1 = 2.329 (2) Å) between the methylated nitrogen atom and the iron(II) atom. The N1 binding energies indicate that the perturbation of the nitrogen atom due to the weaker bond is significant, however, for larger ions of the first transition series (Fe(II) and Mn(II)) and that this perturbation decreases with decreasing size, becoming insignificant for Zn(II).

Introduction

All iron(II) porphyrin complexes previously reported in the literature are readily oxidized by air. Earlier we demonstrated that complexation of manganous ion by an *N*-methylporphyrin (*N*-methyltetraphenylporphyrin or *N*-methyldeuteroporphyrin IX dimethyl ester) results in stabilization of the Mn(II) state relative to the Mn(III) state by nearly 1 V ($E_{1/2}$ = −0.23 V in chloro(tetraphenylporphinato)manganese(III) while $E_{1/2}$ = 0.76 V in chloro(*N*-methyltetraphenylporphinato)manganese(II)[3]). Similar stabilization for Fe(II) was anticipated, and the results of the synthesis, cyclic voltammetry, and molecular structure determination of the air-stable chloro(*N*-methyltetraphenylporphinato)iron(II), [Fe(*N*-CH_3TPP)Cl], are reported herein.

Experimental Section

Synthesis. Chloro(*N*-methyltetraphenylporphinato)iron(II), [Fe(*N*-CH_3TPP)Cl], was prepared by the addition of anhydrous $FeCl_3$ (0.24 mmol) and excess iron wire (0.50 mmol) to dry, distilled,[4] aerated THF (150 mL). The reaction mixture was refluxed under nitrogen for several hours, and *N*-methyltetraphenylporphyrin, prepared from CH_3SO_3F and TPP,[5] was added (0.16 mmol). The solution rapidly turned deep green. After the solution had cooled, a stoichiometric amount of a noncoordinating base, tetramethylpiperidine or 2,6-lutidine, was added. The solution was filtered and allowed to evaporate. The product was repeatedly recrystallized from solutions of dichloromethane and acetonitrile. In solution, [Fe(*N*-CH_3TPP)Cl] is air stable but is readily demetalated by acid to form protonated porphyrin cations.

Cyclic Voltammetry was done in CH_2Cl_2 (dried over a 4-A molecular sieve) with 0.1 M tetrabutylammonium perchlorate (TBAP) recrystallized from methanol as supporting electrolyte. Solutions were deaerated with prepurified N_2 for 15 min prior to the measurements, and N_2 was passed over the solution during the analysis. A three-electrode system was used with a Bio-Analytical Systems CV-1A instrument and a Houston Model 2000 recorder. The working electrode was a Pt-button electrode, the auxiliary electrode was a Pt-wire coil, and a commercial aqueous saturated calomel electrode (SCE), separated from the sample solution by a fiber bridge, was used as the reference electrode. Potentials are reported relative to the aqueous SCE.

Crystal Data. For $Fe(N_4C_{45}H_{31})Cl$: mol wt 719.07, triclinic, a = 7.5620 (6) Å, b = 14.961 (2) Å, c = 17.434 (2) Å, α = 103.15 (1)°, β = 97.124 (9)°, γ = 93.84 (1)°, V = 1896.6 Å^3, ρ_{calcd} = 1.26 g cm^{-3}, Z = 2, $F(000)$ = 744; space group $P\bar{1}$ (No. 2), Mo Kα radiation, λ_1 = 0.709 30 Å, μ(Mo Kα) = 5.2 cm^{-1}.

Data Collection and Reduction. Preliminary Weissenberg and precession photographs revealed only Laue symmetry $\bar{1}$, consistent with the triclinic crystal system. Because the structural studies of the other *N*-methylporphyrin complexes investigated in this series of papers have been completed by using the centrosymmetric space group $P\bar{1}$,[6-9] the same choice was made initially for the present work, and

(1) Colorado State University.
(2) Hunter College.
(3) D. K. Lavallee and M. J. Bain, *Inorg. Chem.*, **15**, 2090 (1976).
(4) D. D. Perrin, W. L. F. Armarego, and D. R. Perrin, "Purification of Laboratory Chemicals", Pergamon Press, London, 1966.
(5) D. K. Lavallee and A. E. Gebala, *Inorg. Chem.*, **13**, 2004 (1974).
(6) O. P. Anderson and D. K. Lavallee, *J. Am. Chem. Soc.*, **98**, 4670 (1976).
(7) O. P. Anderson and D. K. Lavallee, *J. Am. Chem. Soc.*, **99**, 1404 (1977).

0020-1669/80/1319-2101$01.00/0